FUZZY TERMINAL SLIDING MODE CONTROL FOR MAXIMUM POWER POINT TRACKING OF PV CELLS

[1]MOHAMMAD RASOOL MOJALLIZADEH, [2]MOHAMMAD-ALI BADAMCHIZADEH

Faculty of Electrical and Computer Engineering, University of Tabriz
E-mail: mojalli@tabrizu.ac.ir, mbadamchi@tabrizu.ac.ir

Abstract- This paper proposes a fuzzy terminal sliding mode controller (FTSMC) for maximum power point tracking (MPPT) of photovoltaic (PV) power generation systems. Finite time convergence of the proposed system is ensured. The proposed system utilizes a Mamdani fuzzy inference system (FIS) to tune the control gain. As a result, the chattering problem, which exists in classic terminal sliding mode controllers (CSMC), is avoided. A CTSMC is considered in order to compare the results of the proposed system. Simulation results are used to evaluate the robustness of the proposed system. It is shown that the proposed system is robust to system uncertainties, environment changes and load variations.

Index Terms- FTSMC, Sliding mode, Fuzzy, MPPT, PV, Control.

I. INTRODUCTION

Energy issues such as global warming and unstable price of conventional fuels are motivating research on the development of renewable energy resources [1]. Among renewable energies, photovoltaic has attracted a lot of interest because it is free, abundant and environmental friendly [2-4].

In order to extract the maximum amount of PV power, MPPT controllers are developed, such as PI controller [5], passivity-based controller [6], feedback linearization [7] and sliding mode controller (SMC) [8, 9]. Among these controllers, SMC has attracted a lot of interest duo to its robustness to model uncertainty, simple implementation and order reduction [10].

The design of SMC involves two steps: design of the sliding surface, and design of the control signal. The sliding surface is designed based on the control objectives. Consequently, the control signal is designed to ensure the existence condition of sliding mode. Although the transient speed of SMC may be fast, it provides only infinite time convergence. Thus, terminal sliding mode controllers (TSMC) are introduced to ensure the finite time convergence of PV systems [11]. The main drawback of TSMCs is that a trade-off has to be made between the robustness and chattering. Chattering decreases the efficiency of PV systems and may lead those into instability.

The contribution of this paper is in designing a FTSMC for MPPT of PV systems. Compared to the CTSMCs, the gain of control signal is not constant. A Mamdani FIS is utilized to tune the control gain. As a result, not only the chattering amplitude will be suppressed but also robustness of the control system will be improved.

The paper is structured as follows. Modeling of the PV system is presented in section II. The proposed FTSMC is designed in IV. Results of the simulations are given in V. Finally, conclusions are made in VI. Nomenclature of quantities that are used in this paper is shown in Table I.

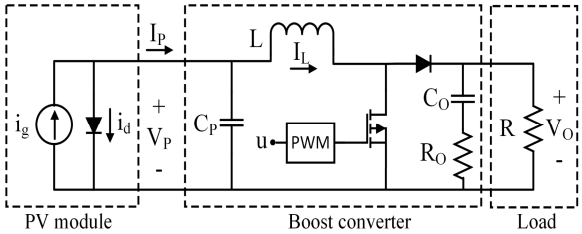


Fig. 1: Schematic of the PV power generation system.

II. PROCEDURE FOR PAPER SUBMISSION

Schematic of the PV system is shown in Fig. 1. The system includes a DC boost converter and a PV module. PV module and DC boost converter are modeled in sections II.A and II.B, respectively.

A. PV module

The characteristic of PV modules can be written as (1), (2) and (3) [8].

$$I_P = N_p\left(i_g - i_d\right) \rightarrow i_d = i_r\left(e^{qV_P/(N_s A K_b T)} - 1\right) \quad (1)$$

$$i_r = i_{or}\left(T/T_r\right)^3 e^{(qE_g)(1/T_r - 1/T)/(K_b A)} \quad (2)$$

$$i_g = (i_s + K_I(T - T_r))\lambda/1000 \quad (3)$$

where, the parameters are defined in Table I. Power characteristic of the PV module is shown in Fig. 2. It can be seen that the maximum power changes along different temperatures. Moreover, a unique V_P exists, which can maximize the PV power.

B. Boost converter

In order to regulate the PV module to its maximum power point (MPP), a boost converter is utilized. The input voltage of the converter can be tuned by its duty cycle. As a result, the converter can change the operating point of the PV module and maximizes the PV power. By using the averaging technique [12], dynamic equations of the PV system can be described by (4)-(6):

$$\dot{V}_P = \left(-I_L + I_P\right)/C_P \quad (4)$$

$$\dot{I}_L = (V_P - R_O(1-u)I_L/(1+R_O/R) + \left(1-u\right)(R_O/\left(R+R_O\right)-1)V_O - V_D(1-u))/L \quad (5)$$

Table I: Nomenclature.

Quantity	Comment
PV module	
λ	insolation level (W/m^2)
T	temperature (K)
i_{or}	reverse saturation current (5.98 × 10^{-8} A)
i_g	light-generated current (A)
i_r	reverse saturation current (A)
i_s	short-circuit current (3.45 A)
A	ideality factor (1.12)
q	charge of an electron (1.6 × 10^{-19})
E_g	band-gap energy (1.2 ev)
K_l	temperature coefficient (12 × 10^{-4} A/K)
K_b	Boltzmann's constant (1.3805 × 10^{-23} J/K)
T_r	reference temperature (298 K)
N_p	number of parallel PV cells (1)
N_s	number of series PV cells (36)
V_{Pd}	MPP voltage (V)
I_P	current of module (A)
V_P	voltage of module (V)
Converter	
R	load resistance (Ω)
C_P	input capacitance (100 μF)
C_O	output capacitance (500 μF)
L	inductance (1.5 mH)
V_D	forward voltage (0.7 V)
R_O	internal resistance of C_O (0.2 Ω)
I_L	inductor current (A)
V_O	Output voltage

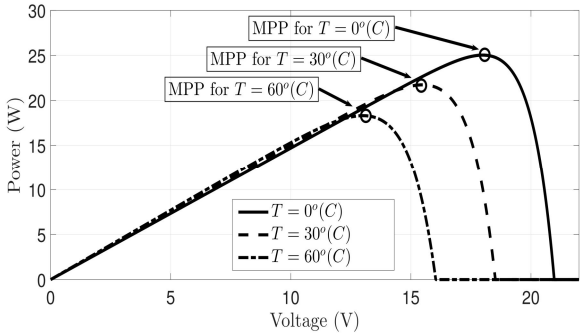


Fig. 2: Characteristic of the PV module under different temperatures. MPPs are shown with circles. (λ=900 W/m^2)

$$\dot{V}_O = \frac{1-u}{C_L(1+R_O/R)}I_L - \frac{1}{C_L(R+R_O)}V_O \quad (6)$$

where, u is duty cycle of PWM signal and can be considered as the control signal. Other parameters are defined in Table I. By considering $x=[V_P, I_L\ V_O]^T$, (5) and (6) can be rewritten as follows:

$$\dot{I}_L = f_1(\mathbf{x}) + g_1(\mathbf{x})u(t) \quad (7)$$

$$\dot{V}_O = f_2(\mathbf{x}) + g_2(\mathbf{x})u(t) \quad (8)$$

where,

$$f_1(\mathbf{x}) = \frac{V_P}{L} - \frac{R_O}{L(1+R_O/R)}I_L + \frac{1}{L}(\frac{R_O}{R+R_O}-1)V_O - \frac{V_D}{L}, \quad (9)$$

$$g_1(\mathbf{x}) = -\frac{R_O}{L(1+R_O/R)}I_L - \frac{1}{L}(\frac{R_O}{R+R_O}-1)V_O + \frac{V_D}{L} \quad (10)$$

$$f_2(\mathbf{x}) = \frac{1}{C_L(1+R_O/R)}I_L - \frac{1}{C_L(R+R_O)}V_O \quad (11)$$

and

$$g_2(\mathbf{x}) = -\frac{1}{C_L(1+R_O/R)}I_L \quad (12)$$

Since the output power of PV modules can be maximized by a specific voltage V_{Pd}, the control objective is to design a control law u such that V_P tracks the V_{Pd}. In this context, a FTSMC will be proposed in the next section.

III. DESIGN OF THE FUZZY TERMINAL SLIDING MODE CONTROLLER

The tracking error is defined as follows:

$$e_1 = V_P - V_{Pd} \quad (13)$$

From (4), (13) can be written as (14).

$$\dot{e}_1 = (-I_L + I_P)/C_P - \dot{V}_{Pd} \quad (14)$$

where V_{Pd} is the MPP reference which is determined using an Adaptive P&O (APO) algorithm. The auxiliary tracking error $e_2 = I_L - I_{Ld}$ with $I_{Ld} = I_P - C_P\dot{V}_{Pd}$ is defined. Therefore, the error dynamics equation can be written as:

$$\begin{cases}\dot{e}_1 = -e_2/C_P \\ \dot{e}_2 = f_1(\mathbf{x}) + g_1(\mathbf{x})u(t) - \dot{I}_{Ld}\end{cases} \quad (15)$$

By (15), the control problem turns into designing the control law u to achieve the finite-time convergence of e_1 and e_2. To this end, a new nonlinear sliding surface s(t) is defined by (16):

$$s = e_2^d - \eta e_1 \quad (16)$$

where, η>0 and d=m/n. m and n are odd numbers such that: 0<n<m<2n and 1<d<2. During the sliding mode, (16) can be written as follows:

$$e_2 = (\eta e_1)^{1/d} \quad (17)$$

Using (14) and (15):

$$\dot{e}_1 = -(\eta e_1)^{1/d}/C_P \quad (18)$$

Equation (18) can be solved as follows:

$$t = \left(|e_1(0)|^{1-1/d}\right)/\left(\eta^{n/m}(1-1/d)\right) \quad (19)$$

Since $e_2=(\eta e_1)^{1/d}$, the convergence of (15) is achieved in a finite time. Therefore, it can be concluded that e_1 and e_2 converge to the origin in a finite time.

Theorem 1. The following control signal ensures the existence condition ($s\dot{s} < 0$):

$$u(t) = \left(-\hat{f}_1 + \hat{h} - ksgn(s) - \eta e_2^{2-d}/dC_P\right)/\hat{g}_1 \quad (20)$$

where,

$$f_1 = \hat{f}_1 + \Delta f_1$$
$$g_1 = \hat{g}_1 + \Delta g_1 \quad (21)$$
$$\dot{I}_{Ld} = \hat{h} + \Delta h$$

where, $\hat{f}_1$, $\hat{g}_1$ and $\hat{h}$ are measurable and Δf_1, Δg_1 and Δh are the measurement errors.

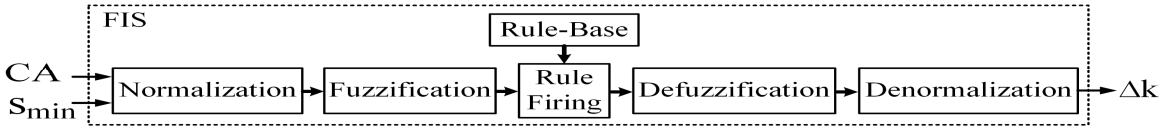


Fig3. Block diagram of the FIS.

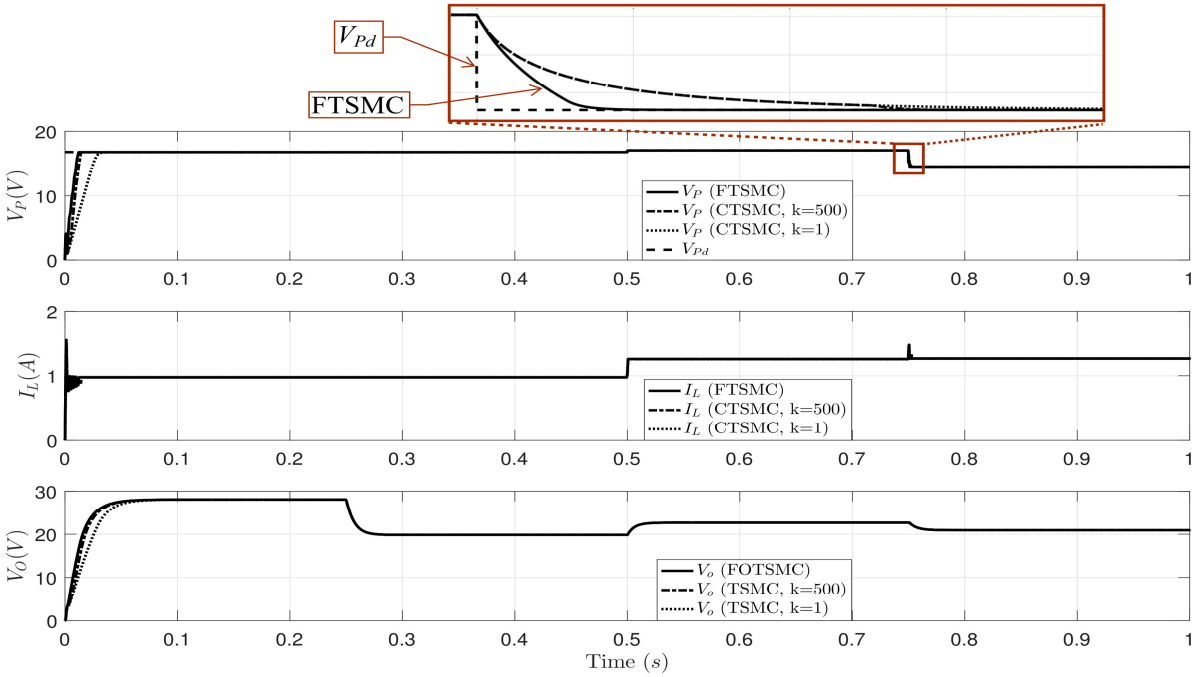


Fig. 4: State-space variables.

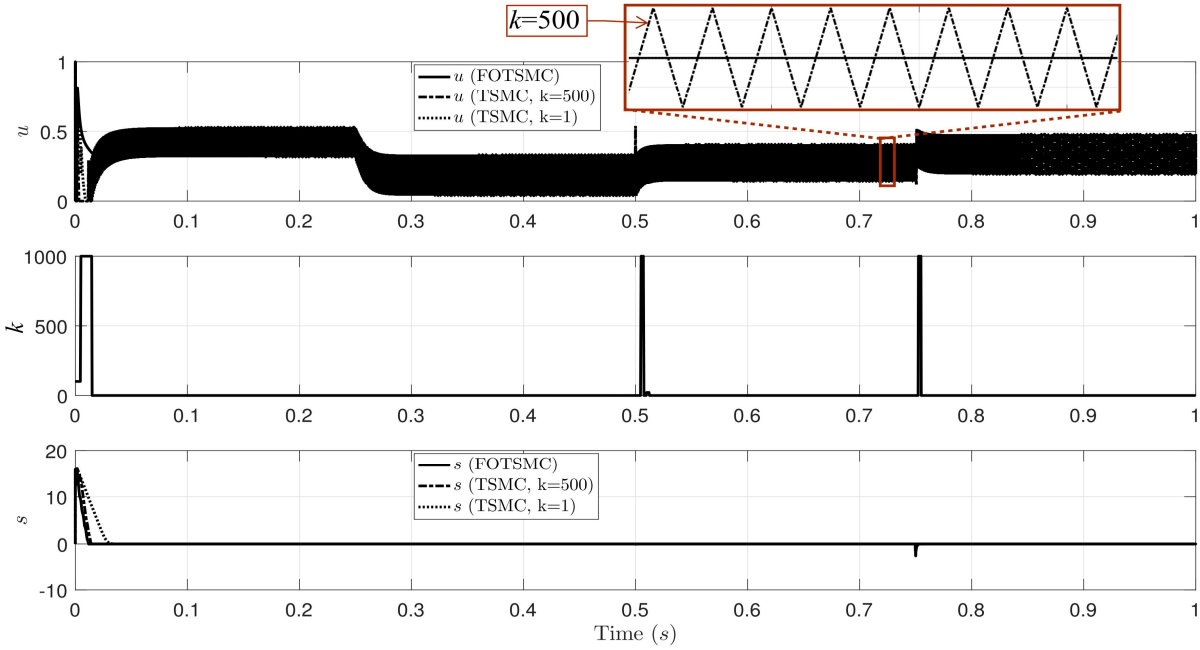


Fig. 5: Control signal (u), Control gain of the FTSMC k) and Sliding surface (s).

The control gain (k) can be designed as follows:

$$k = w\,(|\Delta f_1| + |\Delta h| + c) + |w - 1|\left(\eta\,|e_2^{2-d}|/dC_P + |\hat{f}_1| + |\hat{h}|\right) \quad (22)$$

where,

$$w^{-1} \le \hat{g}_1 / g_1 \le w \quad (23)$$

Proof. The proof of this theorem is presented in [11].

Remark. Since (22) depends on the system uncertainties Δf_1, Δg_1 and Δh, it cannot be used for calculating the appropriate control gain (k). Large amount of control gain results in an unacceptable chattering. Moreover, small amounts of k degrades the robustness of the control system. In this context, a Mamdani FIS is used to tune the control gain. The FIS is designed based on the following observations:

- If the control gain is higher than the optimum gain, the chattering amplitude (CA) will be increased. Therefore, the gain should be decreased to suppress the chattering and improve the steady-state responses.
- Small amount of control gain increase the duration of the reaching-mode. Thus, the gain should be increased to improve the robustness and transient responses of the system.

Block diagram of the proposed FIS is shown in Fig 3. Input variables of the FIS can be calculated as follows:

$$\begin{cases} CA = Max\left(u(t)\right) - Min\left(u(t)\right) \\ s_{min} = Min\left(|s(t)|\right) \end{cases} \quad t \in [t_i, t_i + T) \qquad (24)$$

where, t_i is the initial time and T is the length of the tuning interval. At the end of each interval, output of the FIS is calculated and the control gain is tuned by $k(t_i + T) = \Delta k + k(t_i)$. Blocks of the FIS, which is shown in Fig. 3 are described as follows:

- Normalization block: input variables are multiplied by normalization coefficients. Normalization coefficient of the CA and s_{min} are n_1 and n_2, respectively.
- Fuzzification block: crisp inputs are fuzzified using the Gaussian membership function ($y(x) = e^{\frac{-(x-c)^2}{2\sigma^2}}$).
- Rule firing: fuzzy output is inferred based on the fuzzy rules.
- Defuzzification: crisp outputs are calculated using the center of gravity approach.
- Denormalization block: effect of the normalization is eliminated by multiplying the crisp output by a coefficient (n_3) [13].

The following linguistic fuzzy sets are employed to describe the input variables:

Large (L) (c=1), Moderate (M) (c=2/3), Small (S) (c=1/3) and Zero (Z) (c=0).

Output variable is described based on the following fuzzy sets:

Positive Large (PL) (c=1), Positive Moderate (PM) (c=2/3), Positive Small (PS) (c=1/3), Zero (ZE) (c=0), Negative Small (NS) (c=-1/3), Negative Moderate (NM) (c=-2/3) and Negative Large (NL) (c=-1). The fuzzy rules are shown in Table II.

Table II: Fuzzy rule-base.

CA / $\lvert s_{min} \rvert$	L	M	S	Z
L	-	-	PM	PL
M	-	-	PS	PM
S	NM	NS	ZE	PS
Z	NL	NM	NS	ZE

IV. SIMULATION RESULTS

The robustness of the proposed system is evaluated through simulation. Conditions are shown in Table III.

Table III: Simulation conditions.

Condition / Interval	R(Ω)	λ(W/m^2)	T(C)
t=[0,0.25)	50	700	10°
t=[0.25,0.5)	25	700	10°
t=[0.5,0.75)	25	900	10°
t=[0.75,1]	25	900	40°

Based on this table, the robustness of the system is evaluated through load, irradiance and temperature variations. Parameters of the controllers are shown in Table IV.

Table IV: Parameters of the controllers.

m=19	n=17	η=1	c=0.1
n_1=3	n_2=2	n_3=100	

A CTSMC [11] is considered to evaluate the performance of the proposed FTSMC. Since the gain of CTSMC is constant, responses of this controller is plotted for two different constant gain (k=500 and k=1). MPP voltage is calculated using an APO algorithm [14]. The state-space variables are shown in Fig. 4. It can be seen that the transient responses of the proposed FTSMC is faster than those of the other controllers. Control signals are shown in Fig. 5. Unlike CTSMC, the proposed FTSMC exhibits a chattering free control signal. From Fig. 5, the control gain of FTSMC is not constant. The Mamdani FIS increases the gain to cope with the uncertainties. Moreover, the gain is decreased in the steady-states to suppress the chattering.

Table V: Simulation results.

Index / Control	CA	Energy (J)	Eff%
CTSMC, k=500	0.31	17.64	97.24
CTSMC, k=1	0.00	17.53	96.64
FTSMC	0.00	18.10	99.8

Compared with CTSMC, the gain of the proposed system is not constant and is determined using a Mamdani FIS. Thus, not only its CA is lower than CTSMC but also it exhibits smoother and faster

responses. The results are summarized in Table V. During the simulation, the maximum extractable energy is 18.14 (J).

Compared with CTSMC, the proposed system extracts higher amount of energy. Therefore, its efficiency is higher than the CTSMC.

V. SIMULATION RESULTS

A Fuzzy terminal sliding mode controller is designed for maximum power point tracking of PV generation systems. Compared to classic terminal sliding mode controllers, the control gain of the proposed system is not constant and is determined using a Mamdani fuzzy inference system. As a result, not only the chattering amplitude is suppressed but also robustness of the control system is improved. The performance of the proposed system is evaluated through simulation. It is shown that the proposed system is robust to irradiance, load and temperature. Moreover, its efficiency is higher than the classic terminal sliding mode controllers.

REFERENCES

[1] A. Ajanovic and R. Haas, "Driving with the sun: Why environmentally benign electric vehicles must plug in at renewables," Solar Energy, vol. 121, pp. 169-180, 2015.

[2] V. Benda, "Photovoltaics towards terawatts. progress in photovoltaic cells and modules," IET Power Electronics, vol. 8, pp. 2343-2351, 2015.

[3] G. Mavromatidis, K. Orehounig, and J. Carmeliet, "Evaluation of photovoltaic integration potential in a village," Solar Energy, vol. 121, pp. 152-168, 2015.

[4] F. Fattori, N. Anglani, and G. Muliere, "Combining photovoltaic energy with electric vehicles, smart charging and vehicle-to-grid," Solar Energy, vol. 110, pp. 438-451, 2014.

[5] M. A. Elgendy, B. Zahawi, and D. J. Atkinson, "Assessment of Perturb and Observe MPPT Algorithm Implementation Techniques for PV Pumping Applications," IEEE Transactions on Sustainable Energy, vol. 3, pp. 21-33, 2012.

[6] M. R. Mojallizadeh and M. A. Badamchizadeh, "Adaptive Passivity-Based Control of a Photovoltaic/Battery Hybrid Power Source via Algebraic Parameter Identification," Photovoltaics, IEEE Journal of, vol. 6, pp. 532-539, 2016.

[7] M. A. Mahmud, H. R. Pota, and M. J. Hossain, "Nonlinear Current Control Scheme for a Single-Phase Grid-Connected Photovoltaic System," IEEE Transactions on Sustainable Energy, vol. 5, pp. 218-227, 2014.

[8] M. R. Mojallizadeh, M. Badamchizadeh, S. Khanmohammadi, and M. Sabahi, "Designing a new robust sliding mode controller for maximum power point tracking of photovoltaic cells," Solar Energy, vol. 132, pp. 538-546, 2016.

[9] M. R. Mojallizadeh, M. Badamchizadeh, S. Khanmohammadi, and M. Sabahi, "Chattering Free Full-Order Terminal Sliding-Mode Control for Maximum Power Point Tracking of Photovoltaic Cells," IET Renewable Power Generation, 2016.

[10] K. D. Young, V. I. Utkin, and U. Ozguner, "A control engineer's guide to sliding mode control," IEEE Transactions on Control Systems Technology, vol. 7, pp. 328-342, 1999.

[11] C.-S. Chiu, Y.-L. Ouyang, and C.-Y. Ku, "Terminal sliding mode control for maximum power point tracking of photovoltaic power generation systems," Solar Energy, vol. 86, pp. 2986-2995, 2012.

[12] P. Ngamkong, P. Kochcha, K. Areerak, S. Sujitjorn, and K. Areerak, "Applications of the generalized state-space averaging method to modelling of DC–DC power converters," Mathematical and Computer Modelling of Dynamical Systems, vol. 18, pp. 243-260, 2012.

[13] A. I. Provotar, A. V. Lapko, and A. A. Provotar, "Fuzzy inference systems and their applications," Cybernetics and Systems Analysis, vol. 49, pp. 517-525, 2013.

[14] Y. Wang, Y. Li, and X. Ruan, "High-Accuracy and Fast-Speed MPPT Methods for PV String Under Partially Shaded Conditions," IEEE Transactions on Industrial Electronics, vol. 63, pp. 235-245, 2016.

★★★